

Optimization of gain in traveling-wave optical parametric amplifiers by tuning the offset between pump- and signal-waist locations

Gideon Alon,¹ Oo-Kaw Lim,¹ Amar Bhagwat,¹ Chao-Hsiang Chen,¹ Muthiah Annamalai,² Michael Vasilyev,² and Prem Kumar^{1,*}

¹Center for Photonic Communication and Computing, Electrical Engineering and Computer Science Department, Northwestern University, 2145 Sheridan Road, Evanston, Illinois 60208, USA

²Department of Electrical Engineering, University of Texas at Arlington, Arlington, Texas 76019, USA

*Corresponding author: kumarp@northwestern.edu

Received December 17, 2012; revised February 22, 2013; accepted March 8, 2013;
posted March 13, 2013 (Doc. ID 181758); published April 4, 2013

We present experimental demonstration and modeling of the optimization of a phase-sensitive optical parametric amplifier by tuning the relative position between the pump and signal beam waists along the propagation direction. At the optimum position, the pump beam focuses after the signal beam, and this departure from colocated waists increases with increasing pump power. Such optimization leads to more than 3 dB improvement in the measured deamplification response of the amplifier. © 2013 Optical Society of America

OCIS codes: 190.4410, 230.4320, 230.7020.

Optical parametric amplifiers (OPAs) are ubiquitous these days both in pure research and in industrial applications. Hence, it is important to adjust these OPA systems for optimum matching with the input signal and detector modes. In squeezing experiments, a matched local-oscillator that properly extracts the distorted spatiotemporal squeezed mode can optimize the detected amount of squeezing [1]. In the same spirit, we report here on the performance optimization of an OPA-based system by adjusting the longitudinal offset between the waist locations of the pump and signal beams. We find that the optimal offset is significantly different from zero, contrary to conventional wisdom.

In Fig. 1, we show the key elements of the experimental setup. Light from a telecom-band (1560 nm) continuous-wave distributed-feedback laser is fed into a pulse carver that outputs an 8 MHz train of 160 ps flattop pulses. These pulses are subsequently amplified by a series of erbium-doped fiber amplifiers to reach peak powers of >2 kW. This pulsed, vertically polarized light is then collimated into a free-space beam and focused into a 1 cm long periodically poled potassium titanyl phosphate (PPKTP) crystal for second-harmonic generation (SHG). Conversion efficiencies of >65% produce a pulse train at 780 nm with >1 kW peak power that is then used to pump a 3 cm long PPKTP-based OPA stage. A small signal to be amplified by the OPA is tapped from the main beam prior to the SHG stage, because after the SHG stage, the spatiotemporal mode at 1560 nm is severely distorted due to the high conversion efficiency. Both crystals (Raicol Crystals Ltd.) are poled for type-0 interaction (i.e., all fields are copolarized). The OPA stage is operated as a degenerate OPA. Each of the crystals is held at the phase-matching temperature with better than 10 mK stability. The pump and signal beams are combined on a dichroic mirror (DM) and are directed into the OPA crystal. The focusing lens of the pump beam is mounted on a micrometer-controlled translation stage, allowing for fine adjustment of the pump waist location inside the crystal along the propagation direction. A tap is

placed before the crystal, which directs both beams to a spatial profiler (DataRay Inc., model BMS2-CM4-IGA) capable of measuring beam waists down to 1 μm with 0.1 μm accuracy and the focal-point positions with $\pm 1 \mu\text{m}$ repeatability. The profiler is placed near the focal plane and is used to determine the locations and values of both Gaussian beams' waists in free space prior to measuring the OPA gains. The pump and signal waists are measured to be $(a_0^{px}, a_0^{py}, a_0^{sx}, a_0^{sy}) = (27.1, 25.8, 36.8, 38.6) \mu\text{m} \pm 2 \mu\text{m}$ with a_0 being the $1/e$ intensity radius, which display an approximate $\sqrt{2}$ relationship between the signal and pump waists. Parametric gain and degain values are then measured for various positions of the pump lens via direct detection of the signal beam with a pulse-resolving detector having a bandwidth of 12.5 GHz. The distance along the propagation direction between the waists of the pump and signal beams in the crystal, referred to as the z offset, is inferred by multiplying the translation-stage micrometer readings by the refractive index of the crystal. A piezo-driven mirror controls the relative optical phase between the signal and pump beams. Throughout data collection, the signal beam's waist is not adjusted.

To model the expected gain/degain performance, an implementation of the beam-propagation method using fast Fourier transform (BPM-FFT) is employed. In this method, the continuous-wave field inside the crystal is

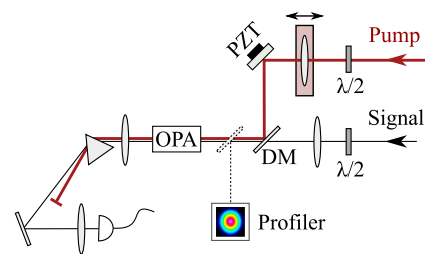


Fig. 1. (Color online) Experimental configuration of the OPA. PZT, piezoelectric transducer; DM, dichroic mirror; $\lambda/2$, half-wave plates.

modeled in discrete symmetrized steps of length h . An initial free-space propagation step of length $h/2$ is followed by diffraction-free nonlinear interaction over a step of length h , which is followed further by a free-space step of length $h/2$. The free-space propagation part of the degenerate phase-matched nonlinear paraxial Helmholtz equation for the signal field \mathcal{E} ,

$$\frac{d\mathcal{E}(\bar{\rho}, z)}{dz} + \frac{1}{2ik} \nabla_{\perp}^2 \mathcal{E}(\bar{\rho}, z) = K\mathcal{E}^*(\bar{\rho}, z)\mathcal{E}_P(\bar{\rho}, z) \quad (1)$$

with $K = i\omega_s\chi^{(2)}/n_s c$ and Gaussian pump field \mathcal{E}_P , is solved in the Fourier domain by a simple multiplication, where the operator ∇_{\perp}^2 reduces to a factor $-(k_x^2 + k_y^2)$ with k_j being the angular spatial frequency, $j = x, y$. The nonlinear part is solved at each iteration step by using the thin-crystal solution (i.e., point-by-point amplification)

$$\begin{aligned} \mathcal{E}(\bar{\rho}, z_{n+1}) &= \mathcal{E}(\bar{\rho}, z_n + h_1) \cosh[\kappa(\bar{\rho}, z_n + h_1)h] \\ &+ ie^{i\varphi_P(\bar{\rho}, z_n + h_1)} \sinh[\kappa(\bar{\rho}, z_n + h_1)h] \mathcal{E}^*(\bar{\rho}, z_n + h_1), \end{aligned} \quad (2)$$

where $\chi^{(2)} = 2d_{\text{eff}}/n_s c$, $h_1 = h/2$, $\varphi_P(\bar{\rho}, z) = \arg[\mathcal{E}_P(\bar{\rho}, z)]$, and $\kappa(\bar{\rho}, z) = \frac{2\omega_s d_{\text{eff}}}{n_s c} |\mathcal{E}_P(\bar{\rho}, z)|$. The residual pump-signal phase fluctuations $\Delta\theta$ that average out the phase-sensitive gain and degain performance of the OPA are included by writing the gain as

$$G(\Delta\theta) = G \cos^2 \Delta\theta + G^{-1} \sin^2 \Delta\theta. \quad (3)$$

In Fig. 2, we show the degain behavior as a function of the pump power. A clear advantage (i.e., greater degree of deamplification) is found for choosing a z offset of

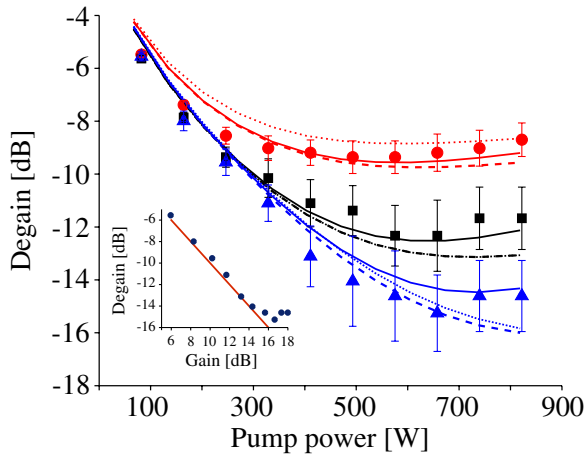


Fig. 2. (Color online) Gain as a function of pump power for different z offsets. Red circles show experimental results for z offset of +5.5 mm (signal waist is downstream from the pump waist). Black squares are data for z offset = 0 mm and blue triangles are data for z offset = -3.7 mm. Results from the model: dotted lines are obtained by scanning the signal waist, dashed lines by scanning the pump waist, and solid lines by scanning the pump waist while including phase fluctuations with $\Delta\theta = 0.65^\circ$. The d_{eff} parameter is used to scale the horizontal axis of the modeled gain for best fit and is found to be 6.3 pm/V. Inset shows degain as a function of gain for z offset = -3.7 mm. Straight line has 1:1 slope.

-3.7 mm compared to colocated waists (i.e., zero offset). As expected, for larger offsets between the pump and signal waist locations, significant deterioration of the degain is also observed. Considering the confocal length $k_0 a_{0p}^2$ of about 1 cm in these measurements, the amount of offset required for optimal degain is substantial. We compare the experimental performance with predictions of the above BPM-FFT model for the case where the pump waist location is scanned and the signal waist location is kept fixed (similar to the case in our measurements) and for the case where the signal is scanned and the pump is kept fixed. Figure 3 shows the degain behavior as a function of the z offset for various pump powers. The beam propagation is from left to right, where negative offset means the signal's waist is located before the pump's in the propagation direction. Clear advantage for negative offsets is observed in both the experiments and models, where the departure from colocated waists increases at higher powers. At the highest pump power shown, with z offset tuning, a degain enhancement of more than 3 dB is observed over the case with zero z offset.

Gain-induced diffraction [2] in traveling-wave OPA distorts the signal wavefront so that some portions of it are in phase for gain while other portions get phased for degain. This behavior degrades the overall phase-sensitive amplifier (PSA) performance in direct detection, particularly for the degain quadrature, because the measured signal power is integrated over the entire wavefront. Fine tuning of the z offset finds the best spot where, in the more critical case of degain, the largest portion of the wavefront is matched for deamplification. We note here that the waist sizes in our experiment are very close to the fundamental eigenmode-0 supported by the PSA (>98% overlap for low pump powers and over 92% at high powers). Exciting orthogonal uncorrelated eigenmodes at the input to an OPA that independently experience degain (or squeezing) [3] can circumvent mode mixing

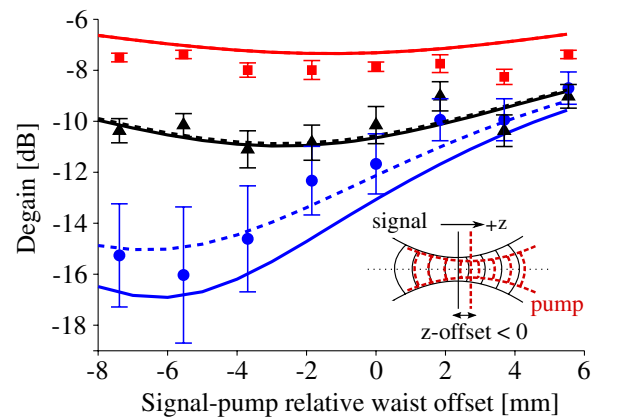


Fig. 3. (Color online) Degain dependence on z offset for pump power of 165 W (red squares), 330 W (black triangles), and 820 W (blue circles). Solid lines are results of simulations obtained by scanning the pump waist. Broken lines are similar to the solid lines but with inclusion of $\Delta\theta = 0.65^\circ$. Inset shows our sign convention of the z offset along the propagation direction. Red broken line is the pump and black thin line is the signal. Negative offset is defined when the pump waist is located after the signal waist.

and gain-induced diffraction [2,4], which is especially critical for measuring large degain (or squeezing) values. By using the optimum z offset, one can improve matching of the wavefront curvature to the eigenmode 0, resulting in even better overlap, especially at high pump powers. This is evident from the relatively high levels of classical degain observed in our traveling-wave experiment, which are within 2 dB of the observed classical gain values (cf. Fig. 2 inset). At such high degain values, phase fluctuations play an important role as indicated by the larger error bars on the high degain data in Figs. 2 and 3. Note also that the model curves in Fig. 2 fit the data better when a small amount of $\Delta\theta$ is taken into account via Eq. (3). Although these measurements were done with classical fields, we anticipate that z offset tuning would carry over to the quantum case, providing enhanced squeezing performance for a fundamental Gaussian mode as well [3,5,6].

Figure 4 shows the modeled evolution of the signal beam's half-width $a_s(z)$ [Fig. 4(a)] and radius of curvature $R(z)$ [Fig. 4(b)] as functions of position z inside the crystal. The solid lines are for the fundamental Gaussian beams of the same waists but with different z offsets in the absence of parametric gain. The symbols show evolution of the same beams in the presence of a parametric pump, as well as the fundamental eigenmode 0. It is clear from Fig. 4(a) that parametric pumping extends the region wherein the beam width is close to the minimum (bottoms of the curves are flattened). This is because the spatially varying gain profile narrows the signal beam's width at the earlier stages of propagation and then limits the diffractive broadening of the signal to that of the pump at the later stages. The reciprocity principle [6] states that the eigenmode 0 profile at the crystal output should be the conjugate of that at the input. A fundamental Gaussian mode with waist $a_s = 36 \mu\text{m}$ and z offset of -2.8 mm has the best overlap (99.2%) with the eigenmode 0 at the input (whereas the one with zero z offset only has 97.2% overlap). This means that the same mode but with an offset of $z = +2.8 \text{ mm}$ has the best overlap with the eigenmode 0 at the output of the crystal. That is, to an outside viewer, the eigenmode 0 at the input appears as a Gaussian beam with a waist before the crystal center, but at the output it appears as a Gaussian beam with a waist after the crystal center. Figure 4(b) confirms this observation by showing that the beam with $z = +2.8 \text{ mm}$ offset has a curvature radius close to that of the eigenmode 0.

In conclusion, we have experimentally demonstrated and confirmed via modeling that an OPA's performance using classical fields as input can be significantly improved by judiciously tuning the z offset between the waist locations of the pump and signal beams. We have also shown that with appropriate z offset, it is possible to approach the fundamental eigenmode of the PSA, making z offset another parameter at an experimenter's disposal for optimizing the PSA performance in various

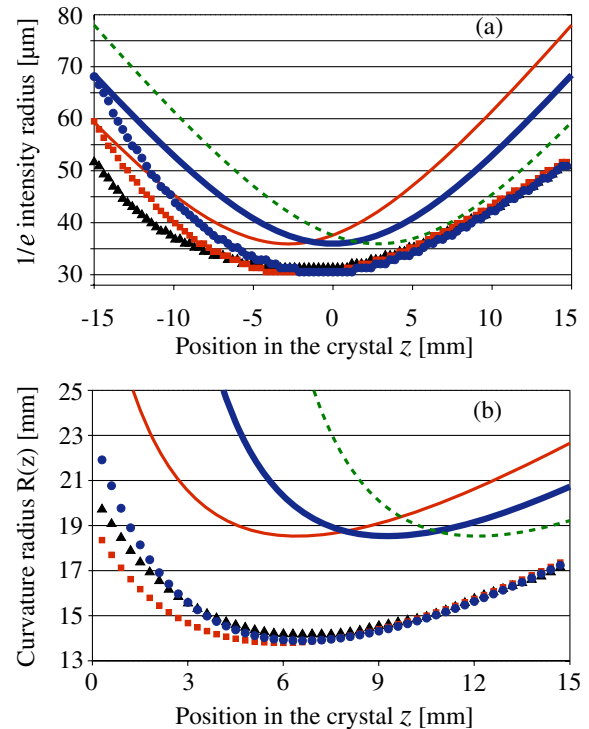


Fig. 4. (Color online) Results from BPM-FFT modeling for the evolution of the signal beam's (a) half-width and (b) curvature radius in the absence (lines) and presence (symbols) of the pump with waist $a_p = 26 \mu\text{m}$ and power $P_0 = 450 \text{ W}$, corresponding to a PSA gain of $\sim 13.8 \text{ dB}$. Red squares and thin line are for a fundamental Gaussian input with -2.8 mm offset; blue circles and thick line are for same input, but with 0 mm offset; green broken line is same input but with $+2.8 \text{ mm}$ offset; and black triangles are the eigenmode 0.

applications. Such enhancement should also translate into the quantum case, where squeezed vacuum would be detected by homodyne detection with a local oscillator having the corresponding waist offset [6].

This material is based upon work funded by DARPA's Quantum Sensor Program, under AFRL Contract No. FA8750-09-C-0194. Any opinions, findings and conclusions or recommendations expressed in this material are those of the authors and do not necessarily reflect the views of DARPA or the U.S. Air Force.

References

1. C. H. Kim and P. Kumar, *Phys. Rev. Lett.* **73**, 1605 (1994).
2. S. K. Choi, R. D. Li, C. H. Kim, and P. Kumar, *J. Opt. Soc. Am. B* **14**, 1564 (1997).
3. M. Vasilyev, M. Annamalai, N. Stelmakh, and P. Kumar, *J. Mod. Opt.* **57**, 1908 (2010).
4. R. D. Li, S. K. Choi, and P. Kumar, *Quantum Semiclass. Opt.* **7**, 705 (1995).
5. M. Annamalai, N. Stelmakh, M. Vasilyev, and P. Kumar, *Opt. Express* **19**, 26710 (2011).
6. K. G. Köprülü and O. Aytür, *Phys. Rev. A* **60**, 4122 (1999).